JOURNAL OF Applied Polymer SCIENCE

Assessment of Resin Formulations and Determination of the Formaldehyde to Urea Molar Ratio by Near- and Mid-Infrared Spectroscopy and Multivariate Data Analysis

Nuno Costa,[1] Sandrina Amaral,[1] Ricardo Alvim,[1] Miguel Nogueira,[1] Manfred Schwanninger,[2] José Rodrigues[3]

[1]EURORESINAS, Plataforma Industrial de Sines Lote Industrial I, 7520-064 Sines, Portugal

[2]Department of Chemistry, BOKU, University of Natural Resources and Life Sciences Vienna, Muthgasse 18, A-1190 Vienna, Austria

[3]Tropical Research Institute of Portugal, Forest and Forest Products Centre, Tapada da Ajuda, 1349-017 Lisboa, Portugal

Correspondence to: M. Schwanninger (E-mail: Manfred.Schwanninger@boku.ac.at)

ABSTRACT: The molar ratios of formaldehyde (F) to urea (U) of three resin formulations in the range from 0.90 to 1.49 have been analyzed by means of Attenuated Total Reflection-Fourier Transform Infrared (ATR-FTIR) spectroscopy and Fourier Transform-Near-Infrared (FT-NIR) spectroscopy. Application of Principal Component Analysis (PCA) to the spectra (MIR and NIR) allowed to separate them according to the molar ratio and to distinguish between two groups of resins. Soft Independent Modeling of Class Analogy (SIMCA) allowed classification of new resin samples with high model distances between the classes. Partial Least Squares Regression (PLS-R) models based on MIR (NIR) spectra resulted in high coefficients of determination (R^2) values, low errors, and high residual prediction deviations (RPD). To confirm the reproducibility of the process and to carefully evaluate twice all multivariate analysis results obtained, different batches of resins have been prepared to have an additional independent sample set. The number of samples required for MIR and possible applications of MIR and NIR spectroscopy in this context including limitations have been discussed. © 2012 Wiley Periodicals, Inc. J. Appl. Polym. Sci. 000: 000–000, 2012

KEYWORDS: infrared spectroscopy; urea-formaldehyde resins; soft independent modeling of class analogy (SIMCA); principal component analysis (PCA); partial least squares regression (PLS-R)

Received 17 April 2011; accepted 13 June 2012; published online

DOI: 10.1002/app.38206

INTRODUCTION

Formaldehyde-based resins, the most common wood adhesives nowadays, are based on reactions of formaldehyde with phenol, resorcinol, urea, melamine, or mixtures thereof.[1] Urea-formaldehyde (UF) adhesives have strong positive aspects: very low cost, nonflammability, very rapid cure rate, and a light color. On the negative side, the bonds are not water-resistant and formaldehyde continues to evolve from the adhesive. UF adhesives are the largest class of amino resins, and are the predominant adhesives for interior grade plywood and particleboard.[1]

Although UF adhesives are known for and used since many years, new formulations for their synthesis are still being based, mostly, on trial and error experiments, due to many different factors that affect the synthetic pathway, which are sometimes difficult to control and accurately reproduce, and the difficulties associated with the analysis (labor intensive, time consuming, expensive) of the intermediate and final products. Kumlin and Simonson have intensively studied the reactions and formations of addition products as well as the condensation products of urea formaldehyde resins.[2–5] Christjanson et al.[6] investigated in detail the structure formation in urea-formaldehyde resin synthesis with NMR. Overall, these studies demonstrate that a great variety and diversity of UF structures, leading to resins with different performance, can be produced by manipulating the synthetic conditions.

FTIR (MIR, 4000−400 cm^{-1}) is a well-known powerful analytical tool to detect functional groups by measuring fundamental molecular vibrations,[7] especially carbonyl groups (e.g., amide bonds) that have a high molar absorptivity can be seen easily, even at low contents. However, although being nondestructive, using ATR devices coupled with a mid-infrared (MIR) instruments is, until now, normally not used for on-line (in-line) process control under conditions found in an industrial

environment. This might be due to three facts or problems: (i) MIR fiber optic ATR probes are usually made with a length of 1–2 m (although available up to 5 m), (ii) the wavenumber range of the probe depends on the material (chalcogenide glass probe for use from 6500 to 1700 cm^{-1} and polycrystalline Silver halide probe for use from 2000 to 600 cm^{-1}) and the ATR crystal used (diamond, zinc selenide or zirconium dioxide), and (iii) the still existing problem of fouling of the ATR crystal. Therefore ATR-MIR (ATR-FTIR) is mainly used off-line or at-line. Alternatively, NIR spectroscopy can be used when coupled to a probe with optical fibers that allow for remote and nondestructive operation. Absorption bands in the NIR region (13000–4000 cm^{-1}) arise from overtones and combination bands caused by vibrations of C—O, O—H, C—H, and N—H groups, which have their fundamental molecular vibrations in the MIR region.[7,8] The absorption signals of various constituents are connatural and highly overlapping and therefore in many cases the bands cannot be directly related to the chemical abundance of a single constituent.[9] NIR spectroscopy is a rapid and nondestructive method used for process and quality control in many areas such as food and beverages, agriculture, biotechnology, petrochemistry, pharmaceutical production,[9,10] as well as for research purposes in wood, pulp, and paper science for more than 20 years.[11,12] Although NIR in combination with optical fibers has been used since years for on-line (in-line) process control it is still a challenge to use transmission probes in aqueous systems, because the optical path length is limited to 1 mm, in order to avoid total absorbance in the range of the combination water band at about 5180 cm^{-1}, and due to the fouling problem of the small slit (1 mm) of a transmission probe.

As in various cases, the chemical information is hardly selective within typically broad and extensively overlapping bands of NIR spectra. Multivariate analysis techniques such as PCA have to be used to model data relevant in information for classification (SIMCA) and prediction of wood and waste properties, respectively.[10,13–22]

The production of the urea-formaldehyde adhesives involves several steps, with the first being the addition of the formaldehyde to the urea under neutral or basic conditions,[1] which can be followed by infrared spectroscopy. MIR spectroscopy was already used in 1967 to determine the UF resin content in paper,[23] to study the prepolymer and cured state,[24] the curing reactions,[25] to identify and follow the appearance, increase, decrease, and disappearance of several of the main chemical groups during the preparation of the initial UF phase of the reaction and the subsequent reaction of melamine with the UF resin that was formed.[26] Moreover, it was used to investigate the structure development of UF resins in a synthesis process, and to reveal structural differences of reaction inter-products of urea and formaldehyde that were observed in alkaline and acidic media and at different F/U molar ratios.[27] MIR was also used to investigate the effects of reaction pH condition and hardener type on the reactivity, chemical structure, and molecular mobility of UF resins,[28] as well as for investigations of other adhesives,[26,29–34]

A method based on FT-NIR and chemometrics was developed for the assessment of the pathway(s) followed during formaldehyde-based resin synthesis at both laboratory and industrial scale.[35] They have also made multivariate calibrations for urea and formaldehyde for a wide concentration range. The effect of pH and temperature on the structure of UF resins was monitored by FT-NIR spectroscopy via optical fibers *in situ*,[36] and NIR spectroscopy was used in the production of modified industrial resins.[37] Moreover, a patent on the use of NIR spectroscopy in composite panel production exists.[38]

The aim of this study was to follow and evaluate the production of three UF resins types by infrared spectroscopic methods. The spectra have been collected simultaneously on two infrared spectrometers to avoid possible influences due to aging effects. Besides visual inspection of the spectra multivariate methods were used for evaluation. PCA was used to identify differences between the resins, SIMCA to classify them and PLS-R to determine the formaldehyde to urea molar ratio of UF resin formulations. The results of the PLS-R models based on MIR and NIR data have been compared. All multivariate analysis results have been evaluated by an additional independent sample set. Therefore, in order to proof the reproducibility of the process and to carefully evaluate the obtained results different batches of resins have been prepared independently.

EXPERIMENTAL DETAILS

Materials

Laboratory Resins Synthesis. The urea-formaldehyde (UF) resin samples were produced in a 5-L round bottom flask equipped with a mechanical stirrer and a thermometer (immersed in the solution). A heating mantle controlled the temperature. The flask was charged with formaldehyde, urea, and water and the pH of the initial solution was adjusted with a base (sodium hydroxide). The solution was heated up to the desired temperature, and the pH was readjusted by the addition of an acid. At this point, a second quantity of urea was added to reach the desired molar ratio for the polymerization. When the viscosity had reached a certain value (300–600 mP s), polymerization was terminated by the addition of a base. Finally, the total amount of resin was divided in n parts (13 to 16 parts depending on the resin type, see next paragraph) and a third quantity of urea was added (to each of the n parts) to decrease the molar ratio (MR) to the desired value (production of n samples with different molar ratio) with the final viscosity (150–300 mP s) and pH (8–9.5).

Three types of UF resins were produced, namely R1 (14 (12+2) samples; MR: 0.90–1.10), R2 (16 (13+3) samples; MR: 1.11–1.49), and R3 (13 (10+3) samples; MR: 0.91–1.48). The range was chosen taking into account that the usual molar ratio of this type of resins, when industrially produced, is about 1.1. Each resin type has been prepared twice, e.g., for the 14 samples of R1, 12 samples have been prepared first and then additional two samples have been prepared in a second batch for verification and a second validation of the methods (PCA, SIMCA, and PLS-R) to have an independent test set (TS2).

The resins R1 and R2 are very similar in terms of production as they incorporate the same components; apart from formaldehyde, urea and water, they also have small amounts of

melamine and hexamine in their formulations. The difference between these two resins lies in the value of viscosity at which the polymerization is terminated. Concerning the resin R3, it does not incorporate melamine or hexamine; it is also terminated at a different viscosity value.

Infrared Measurements. FT-NIR spectra were recorded at ambient temperature using a transmission-probe (1 mm optical path length) connected to a Bruker (Bruker Optics, Ettlingen, Germany) FT-NIR process-spectrometer (Matrix-F; TE-InGaAs detector). 100 scans per spectrum (12,000–4000 cm^{-1}) were collected at a spectral resolution of 8 cm^{-1} and a zero filling of 2. Air was used as background. After collection of each spectrum the transmission probe was rinsed at least twice with water and refilled with the new sample also at least twice before spectra acquisition. Two spectra from each sample were collected and averaged.

ATR-FTIR spectra (32 scans per sample, spectral resolution: 4 cm^{-1}, wavenumber range: 4000–400 cm^{-1}) using a diamond single reflection attenuated total reflectance (ATR) device were recorded with a Bruker FT-IR spectrometer (Alpha) and a zero filling of 2 was applied.

Data Processing

Post spectroscopic manipulation was kept to a minimum. The NIR spectra were used as obtained. Atmospheric compensation in the full wavenumber range (4000 to 400 cm^{-1}) and offset-correction to the minimum between 1920 and 1880 cm^{-1} was applied to the ATR - FTIR spectra (Software OPUS 6 from Bruker). The maximum offset of the spectra before offset-correction was very small (0.02 ATR units) compared to the amide-II band at 1540 cm^{-1} (0.90 ATR units), which in principle could be neglected as identical results (not shown) were obtained for all evaluations. Second derivatives of the NIR spectra used to find band positions were obtained applying the Savitzky-Golay[39] algorithm with a 17 points smoothing filter and a second order polynomial.

Multivariate Data Analysis

Principal component analyses (PCA) were performed using OPUS Quant 2 (Bruker) and The Unscrambler Vsn 9.8 (CAMO Software AS., Oslo, Norway). Soft independent modeling of class analogy (SIMCA) was performed with The Unscrambler Vsn 9.8.

Soft Independent Modeling of Class Analogy (SIMCA)—Model Validation and Classification. SIMCA modeling consisted in building one PCA model for each class of the three resin types (R1, R2, and R3) which describes the structure of that class, based on the infrared spectra (either MIR or NIR), as well as possible. The optimal number of principal components (PCs) for each model was chosen separately according to a full cross validation. The samples used CVall (34) and TS2 (8) are described later (see section Calibration models and validation of the models). The MIR spectra in the wavenumber range from 1780 to 880 cm^{-1} and the NIR spectra in the wavenumber range from 10,000 to 4160 cm^{-1} were used without any preprocessing.

Before using the models to predict class membership for new samples, their specificity, i.e., whether the classes overlap or are sufficiently distant to each other was evaluated. The model distance is a measure (called "model-to-model distance") that shows how different two models are from each other. It is computed from the results of fitting all samples from each class to their own model and to the other one. The value of this measure was compared to 1 (distance of a model to itself). A model distance much larger than 1 indicates that the two models are quite different, which in turn implies that the two classes are likely to be well distinguished from each other. Distances of more than 3 indicate a significant segregation between the defined classes.[40]

The Cooman's plot, where the sample-to-model distances are plotted against each other for two models, includes class membership limits (significance level was set to 5%) for both models, so that it can be seen whether a sample is likely to belong to one class, or both, or none. The Cooman's plots used for SIMCA validation were calculated for all class models as well as for the classification of the test set samples (TS2) of each resin formulation.

Partial Least Squares Regression (PLS-R) Modeling. OPUS Quant 2 software was used for data preprocessing (e.g., 1st derivatives + vector normalization) and for the calculation and validation of the PLS-R models. The measured spectra were processed (smoothed and derived) by means of 17-points smoothing filter and a second order polynomial to obtain first derivatives with OPUS software (version 6,). For calibration (cross validation, test set validation), the infrared data sets were regressed against the formaldehyde to urea ratio. The numbers of spectra subjected to PLS-R are indicated in the results and discussion section.

Calibration Models and Validation of the Models. Firstly the data set was divided into two groups (CV and TS1). After sorting the whole data set according to the F/U ratio, about every 5th sample was chosen for the test set (TS1) and the remaining for the calibration set/cross validation set (CV). The preprocessed spectral data were regressed against the formaldehyde to urea ratio and, by full cross validation, a significant number of PLS factors was obtained.[13]

All models were calculated to a maximum of 10 PLS factors and the results of the cross validation (R^2 and RMSECV: root-mean-square-error of cross validation) and the test set validation (R^2 and RMSEP: root-mean-square-error of prediction) were compared. Therefore, test set validation was performed computing the calibration model with the optimal number of PLS factors determined by cross validation (as usual in an external validation), and also an optimal number of PLS factors was defined through test set validation. The optimal number of PLS factors was determined as follows:

1. The number of PLS factors with the smallest PRESS (predictive residual error sum of squares = sum of all squared differences between true and predicted values) value was searched.
2. For all lower numbers of PLS factors, the quotient of their PRESS values and the minimum was calculated ($=F_{value}$).

Applied Polymer SCIENCE

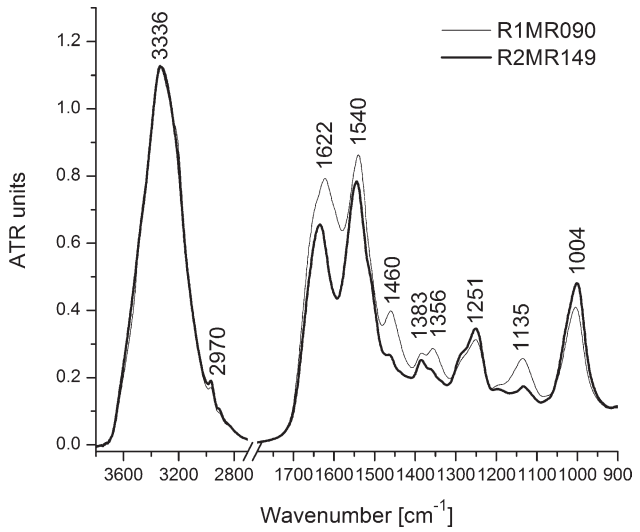

Figure 1. ATR spectra of the resin R1 and R2 with molar ratios of 0.90 and 1.49 respectively covering the full range.

3. From this F value, a probability was calculated [$F_{prob}(F_{value}, M, M)$, where M is the number of samples].
4. The number of PLS factors, having a probability smaller than 0.75 for the first time, was chosen as the optimal number of PLS factors.

The comparison of the number of PLS factors gives a first indication of the predictive ability of the model, because models with large differences between the number of PLS factors determined by CV and TS are never satisfactory.[13,41,42] Thereafter, the CV and TS1 samples were combined giving the CVall sample set for calibration / cross validation, to have a larger sample set covering more spectral variation. These models were evaluated by an additional independent test set (TS2).

The RPD (residual prediction deviation or ratio of performance to deviation) was introduced by Williams and Norris[8] several years ago and is calculated as the ratio of two standard deviations; the standard deviation of the reference data for the validation set and the standard error of prediction (from cross validation or test set validation).

RESULTS AND DISCUSSION

Both techniques (ATR-FTIR and FT-NIR) were investigated for their applicability for classification and prediction of samples covering a wide range as well as a narrow range of F/U molar ratios of different resin formulations.

Spectra in the Mid-Infrared Region (FTIR)

Spectra of the resins R1 with the lowest (0.90) and R2 with the highest (1.49) formaldehyde to urea molar ratio are shown in Figure 1; the position, as well as the assignment of the bands of these samples together with bands found for other samples (R2 and R3) with different MRs, are given in Table I. The intensity of most of the bands decreases with increasing molar ratio and additionally shifts to higher wavenumbers, also described by others.[26,27] They were able to describe the influence of pH (alkaline and acidic media) and different formaldehyde-to-urea molar ratio on the structural difference of reaction inter-products (e.g., ether linkages, methylene linkages, content of methylols and -NHCH$_2$- groups),[27] and to identify and follow the appearance, increase, decrease, and disappearance of several of the main chemical groups during the preparation of the initial urea-formaldehyde (UF) phase of the reaction and the

Table I. Band Positions in the ATR-FTIR Spectra and Their Assignment

Wavenumber (cm^{-1})				
Resin 1 MR 0.90	Resin 2 MR 1.11	Resin 2 MR 1.49	Resin 3 MR 0.91	Band assignment
3336	3335	3331	3338	ν(NH)[7,26,43]
2970	2970	2968	2969	ν_a(CH) of CH$_2$
2901	2901	2901	2901	ν_s(CH) of CH$_2$
1656 sh	1656 sh		1656 sh	ν(C=O) of amide I (urea)[26] and ν(C=N) from the triazine ring of melamine [44]
1622	1629	1635	1620	δ(NH) of amide I (urea) [26]
1540	1542	1544	1539	ν(C—N and N—H) of amide II and secondary amines[25,26,43]
1460	1462	1464	1459	δ(CH$_2$)[25,26,43,45]
1383	1384	1385	1384	γ(CH$_2$)[25,28,43]
1356	1357	1361	1354	ν(C—N)[25,26,28,43]
1290 sh	1290 sh	1290	1290 sh	δ(OH) plus amide III[26,43]
1251	1251	1251	1254	ν(C—N) and ν(N—H) of tertiary amines[7,25,28] and —CH$_2$— of —CH$_2$—O—CH$_2$—[26] and ν_a(C—OH)[32]
1135	1135	1133	1135	ν(C—O) of C—O—C[25,26,28]
1004	1003	1001	1004	ν(C—O) of —CH$_2$OH[28,43,45]

MR, molar ratio; sh, shoulder; a, antisymmetric; s, symmetric.

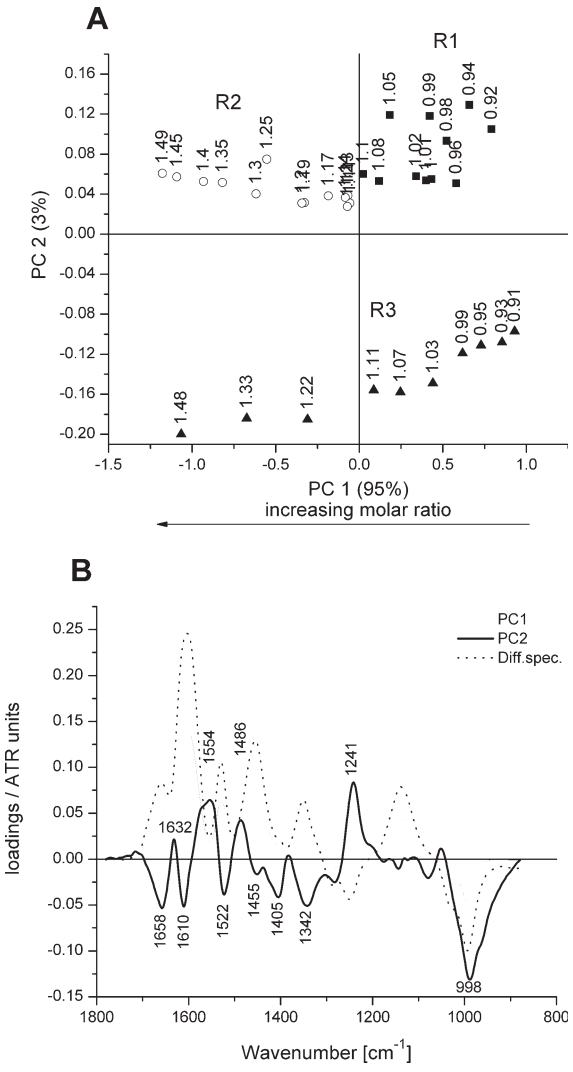

Figure 2. A: Scores plot PC 2 versus PC 1 of all resins MIR spectra in the range from 1780 to 880 cm^{-1}, and the corresponding loadings plots as well as the difference spectrum B). The groups in (A) are labeled according to the resin types (■ R1, ○ R2, and ▲ R3), and the samples according to the molar ratios. The labels of the variables in (B) belong to the PC 2 loadings.

subsequent reaction of melamine with the UF resin that was formed.[26]

A principal component analysis (PCA) performed using the fingerprint region of the MIR spectra from 1780 to 880 cm^{-1} of the CVall samples resulted in a separation of the samples in the PC 1 – PC 2 score plot [Figure 2(A)]. Using the CVall + TS2 sample sets gave the same pattern and loadings (not shown), which confirms that the independent sample set TS2 fits perfectly to those of the CVall sample set. A separation according to the molar ratio appears along PC 1. The corresponding loading plot [Figure 2(B)] shows the variables (bands) responsible for that. The loadings of PC 1 are almost identical with the difference spectrum [Figure 2(B)] of the spectra shown in Figure 1. This was expected because (i) the molar ratio decreases continuously along PC 1, and (ii) most of the variation between the samples is due to the decreasing molar ratio (the increasing urea content), which is expressed by the variance explained by PC 1 (95%).

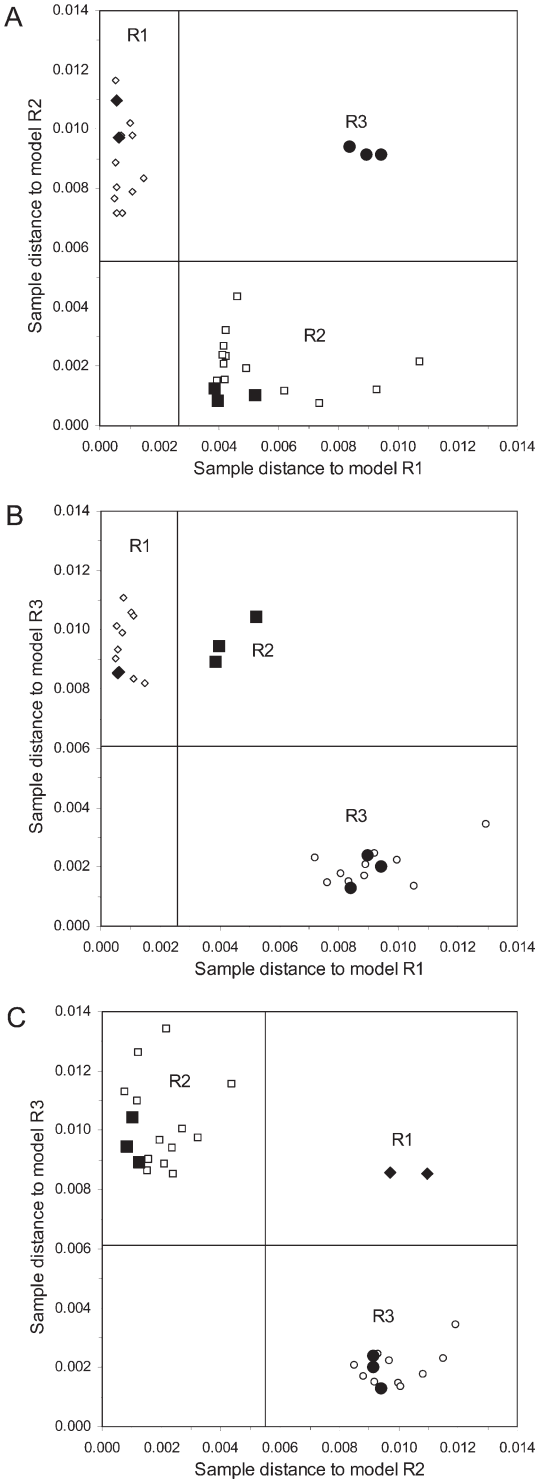

Figure 3. A–C: Cooman's plots of the SIMCA model (3 PCs for R1 and 1 PC each for R2 and R3) for the three resins R1, R2, and R3 based on the MIR spectra in the wavenumber range from 1780 to 880 cm^{-1}. The filled symbols represent the samples used for classification (TS2) on a significance level of 5%. The horizontal and vertical lines in the graphs represent the confidence limits.

Applied Polymer SCIENCE

Along PC 2 the samples were divided into two groups R1 + R2 and R3. The samples of R1 and R2 contain melamine and hexamine that is expressed by the variables (bands) at 1632 cm^{-1} (water and melamine), 1600 cm^{-1} ν_a (C—N amide II),[27] 1554 cm^{-1} (melamine and ν(C—N and N—H) of amide II), 1486 cm^{-1} (urea, melamine, and hexamine) and 1241 cm^{-1} (hexamine) [Figure 2(B)]. On the other hand, the samples of R3 have more of the components represented by the variables (bands) at 1658 and 1610 cm^{-1} from urea, 1522, 1455, 1405, 1342, and 998 cm^{-1}. More urea could mean that the amount of prepolymers is lower in R3 compared with R1 and R2, which is confirmed by the variables at about 1455 and 1160 cm^{-1} (seen in urea and methylene diurea[36]), and the one at 1455 cm^{-1}. The higher formaldehyde content, 1405, 1342,[27] and 998 cm^{-1}, additionally confirms this. The band at 1522 cm^{-1}, N—C—N of a proper methylene bridge (—CH_2—),[26] and two bands around 1455 cm^{-1} at 1470 and 1438 cm^{-1} are assigned, respectively, to the bending mode of methylene units in the N—CH_2—N and in the CH_2—OH structures[31] (which can arrive from dimethylol urea, monomethylol urea, and dimethylol methylene diurea) gives hint to more addition products. Additionally the variables at 998 cm^{-1} supports that more addition products (methylol groups) and less prepolymers were build.[27] Moreover, two poly-condensation steps were performed producing R1 and R2, and only one for R3. The differences in pH, temperature and reaction time influence the ratio between addition products and prepolymers. However, it has to be kept in mind that the spectral differences between the R1 + R2 samples and the R3 samples of the same *F/U* ratio are very small and that the explained variance is only 3%. Therefore the differences in the content of each component, of addition products as well as differences in the prepolymer content can be very small too, which is additionally influenced by pH, temperature, and reaction time during resin preparation. Nevertheless, as identical results were obtained for the PCAs for the CVall and CVall + TS2 sample sets the explained variance of 3% is sufficient to draw the conclusions and confirms that the process is highly reproducible which is a prerequisite for process control.

Classification Using Soft Independent Modeling of Class Analogy (SIMCA) and Model Validation

A separate full cross-validated model was created for each resin requiring 3 PCs for R1 and 1 PC each for R2 and R3 to satisfactorily describe each data set. Models for R1, R2, and R3 explain 99.5%, 98.0%, and 99.5% of the data, respectively. The significance level was set to 5%. The Cooman's plots used for SIMCA validation are shown for all class models as well as the classification of the test set samples (TS2) of each resin formulation (Figure 3). Spectra of the test set samples (TS2) from each resin formulation fall into the membership limits, confirming a correct classification. The distances from SIMCA classes (R1, R2, and R3) to the class R1 are 1 to the class R1, 23 to class R2, and 43 to class R3. The large distances of the established SIMCA confirm the applicability of the MIR spectroscopic pattern to unequivocally distinguish different resin formulations.

Spectra in the Near-Infrared Region (NIR)

The average spectra, as well as the second derivatives of the NIR spectra of the resins R1, R2, and R3, are shown in Figure 4 and

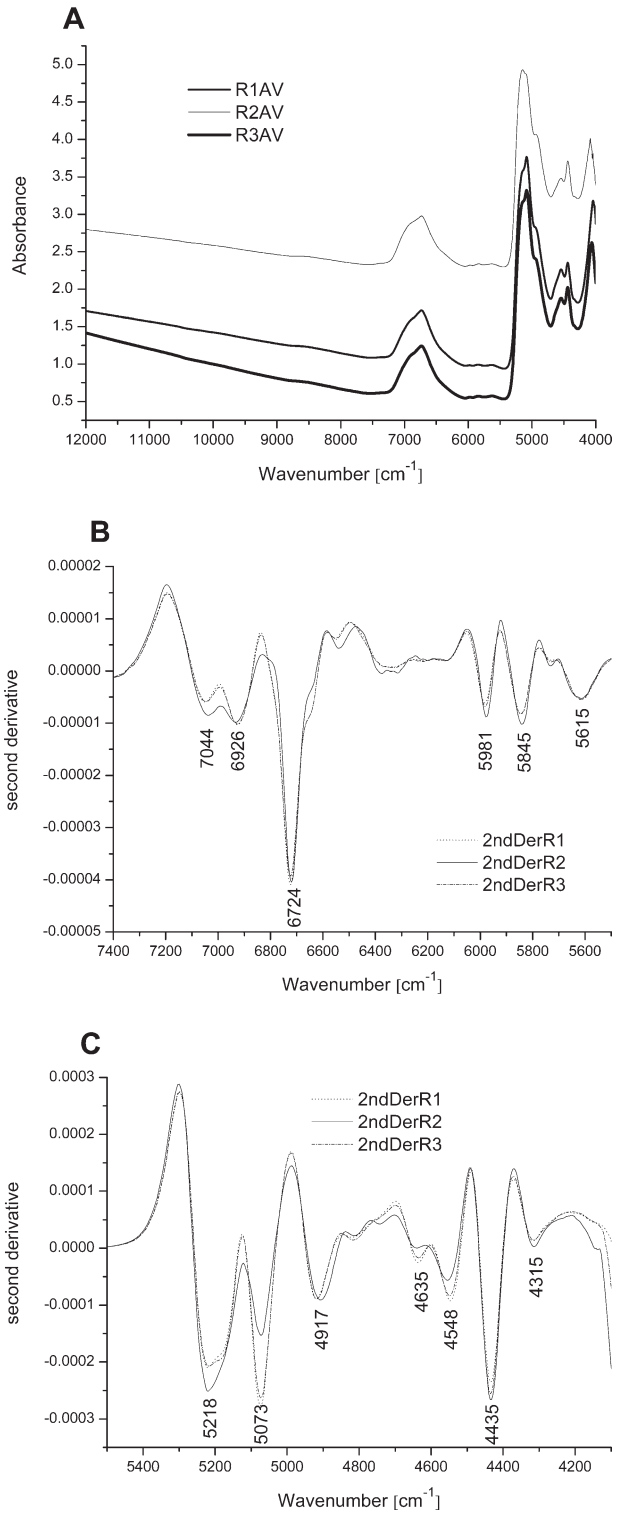

Figure 4. A: NIR average spectra of the resins R1, R2, and R3 from top to bottom and their second derivatives in the wavenumber range B) from 7400 to 5500 cm^{-1} and C) from 5500 to 4100 cm^{-1}.

the position as well as the assignment of the bands, are given in Table II. The obvious baseline differences between the three resin formulations [Figure 4(A)] in increasing order R3 < R1 < R2 seem to be due to different poly-condensation reactions that

Table II. Band Positions Determined from the Second Derivatives of the NIR Average Spectra and Their Assignment

Wavenumber (cm^{-1})			
Formaldehyde 6*M*	Urea 6*M*	R1/R2/R3	Band assignment
	6803		$2\nu_a(NH)$[46]
	6750 sh	6724	$2\nu_s(NH)$[46,36a]
	6668		$\nu_s(NH) + \nu_a(NH)$ comb. band[46]; $2\nu_a(NH_2)$[44] from melamine
	6575		$2\nu_s(NH_2)$[44] from melamine
		5073	$\nu_s(NH_2) + \delta(NH_2)$ comb. band[36,44,b]
	5037		$\nu_s(NH_2) + \delta(NH_2)$ comb. band[36,44,b]
	5035		$\nu_a(NH)$ + amide II[46]
	4952		$\nu_s(NH)$ + amide II[46d] and $\nu_s(NH_2) + \delta(NH_2)$[36, c]
	4824		$\nu_a(NH)$ + amide III[46] should appear at 4808 cm^{-1}
	4644	4635	$\nu_a(NH_2) + \rho(NH_2)$[36,e]
	4546	4548	$\nu_s(NH_2) + \rho(NH_2)$[36,f]
4436		4435	from methanol ??[g]
		4315	$\nu_s(CH) + \delta(CH_2)$ comb. band[36]
4277			from methanol ??[g]

Only the bands labeled in Figure 4 and the bands form formaldehyde and urea are presented in the table. sh, shoulder; s, symmetric; a, antisymmetric; comb, combination band.

[a]Second overtone of the secondary NH bond stretch, indicating the formation of *N, N′* disubstituted amide species, [b]Combination band NH stretching plus NH bending at 5080–4980 cm^{-1}, [c]Combination modes between the N—H stretches bending modes of the NH_2 group, [d]Should appear at 4902 cm^{-1}, [e]Combination modes between the N—H stretches and the rocking of the NH_2 group, [f]Combination modes between the N—H stretches and the rocking of the NH_2 group 4645, 4549; according to Workman[46] $\nu_a(NH_2) + \rho(NH_2)$ should appear at 4505 cm^{-1}.

lead to "larger" (more condensed and branched) reaction products, which scatter a part of the NIR radiation. The changes of bands (intensity and shifts) with decreasing molar ratio were also found by others.[35,36] Dessipri et al.[35] show NIR spectra of increasing urea concentrations as well as of several steps of *F/U* ratios in the combination band range. Moreover, they followed two pH dependencies of the evolution of the reaction progress as indicator for two methylolation reaction and monitored an acid-induced poly-condensation step of a resin synthesis. Kumlin and Simonson[3] also examined the influence of pH, temperature, and F/U molar ratio and showed that the formation of oxymethylenediurea compounds was favored at alkaline pH and increased with increasing pH from 8.0 to 9.4, whereas the formation of diurea compounds containing a methylene bridge was strongly favored when the reaction mixture was made acidic and increased with decreasing pH from 5.1 to 3.5. At low *F/U* molar ratios (from 1.4 to 1.6), a minimum in the formation of condensed products was found at a pH value of about 8, while with increased molar ratio ($F/U = 2.2$) the reaction minimum appeared at neutral pH. In all cases, a high reaction temperature greatly increased the condensation. Minopoulou et al.[36] used NIR for structural characterization of urea–formaldehyde resins and found that the reactions of urea and formaldehyde at different temperatures and pH values result in resins with different structures and properties: Resins produced at high temperatures and acidic pH values exhibit higher degrees of condensation, presumably because of the development of more cross-linked structures. In principle, their findings could be confirmed with the three resin formulations used in the presented study. Some of the bands were differently assigned in the literature (see Table II). Minopoulou et al.[36] also investigated UF model compounds but unfortunately neither NIR spectra nor band assignments were provided.

A principal component analysis (PCA) performed using the region of the 1st derivative + vector normalized NIR spectra from 7502 to 5446 cm^{-1} and 4902 to 4158 cm^{-1} (the same range as used later for the prediction of molar ratio) resulted in a separation of the samples in the PC 1 – PC 2 score plot [Figure 5(A)]. A separation according to the molar ratio appears along PC 1. The corresponding loadings plots [Figure 5(B,C)] show the variables (bands) responsible for that. The loadings of PC 1 in the lower combination band range (4902 to 4158 cm^{-1}) [Figure 5(C)] are mainly dominated by bands representing urea and formaldehyde. This was expected because i) the molar ratio increases continuously along PC 1, and ii) most of the variation between the samples is due to the increasing molar ratio (lower urea content), which is expressed by the variance explained by PC 1 (95%). The PC1 loadings are much smaller in the higher wavenumber range [7502 - 5446 cm^{-1}; Figure 5(B)], whereas at higher frequencies the 2nd overtones as well as the ($\nu_s + \nu_a$) combination modes of the N–H stretches are observed and several weak and sharp features appear in the 5800–5600 cm^{-1} range, where the overtones of the C–H stretching modes are expected. These features change in relative intensity as formaldehyde reacts to methylolate urea, but a more detailed assignment is not currently available. The differences between R1 + R2 and R3 that allow separating them along PC 2 have already been discussed in context with the MIR spectra. Additionally, small differences in the formaldehyde content

Applied Polymer SCIENCE

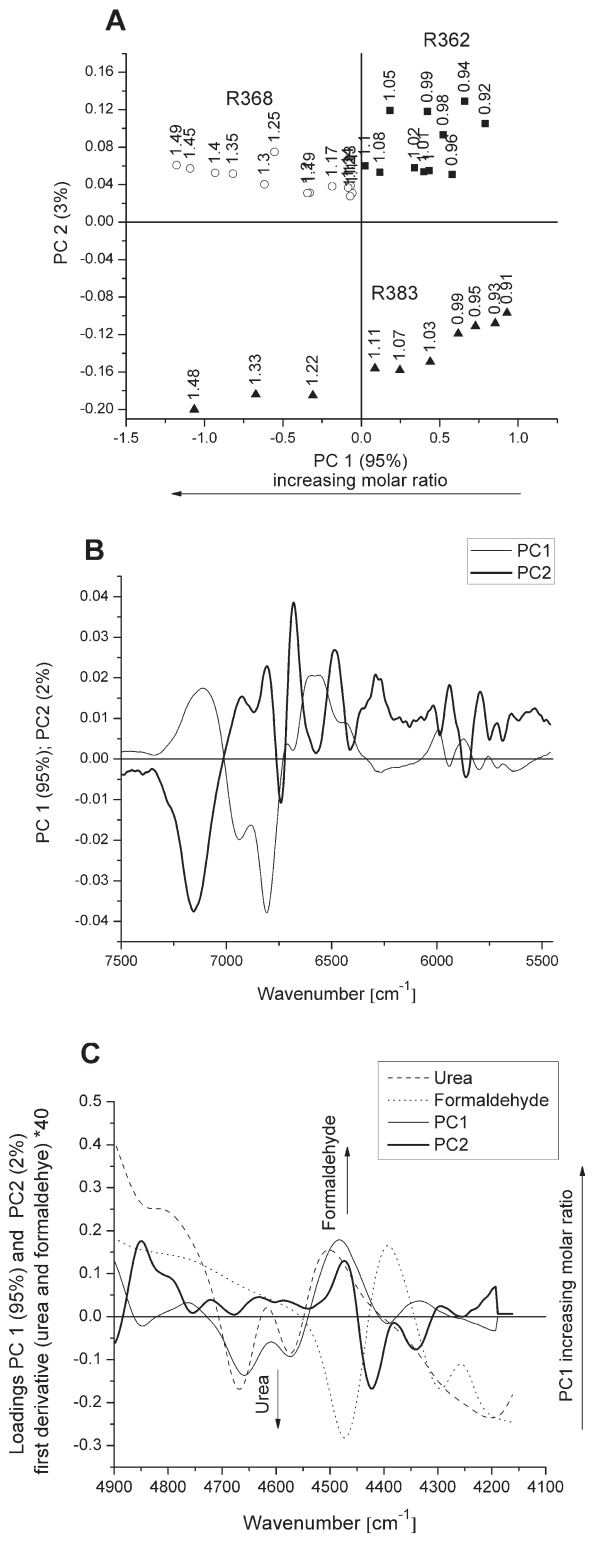

Figure 5. A: Scores plot PC 2 versus PC 1 of all resins NIR average spectra in the ranges from 7502 to 5446 cm^{-1} and 4902 to 4158 cm^{-1}, and the corresponding loadings plots B) in the range from 7502 to 5446 cm^{-1} and C) from 4902 to 4158 cm^{-1}. The groups in (A) are labeled according to the resin types (■ R1, ○ R2, and ▲ R3), and the samples according to the molar ratios.

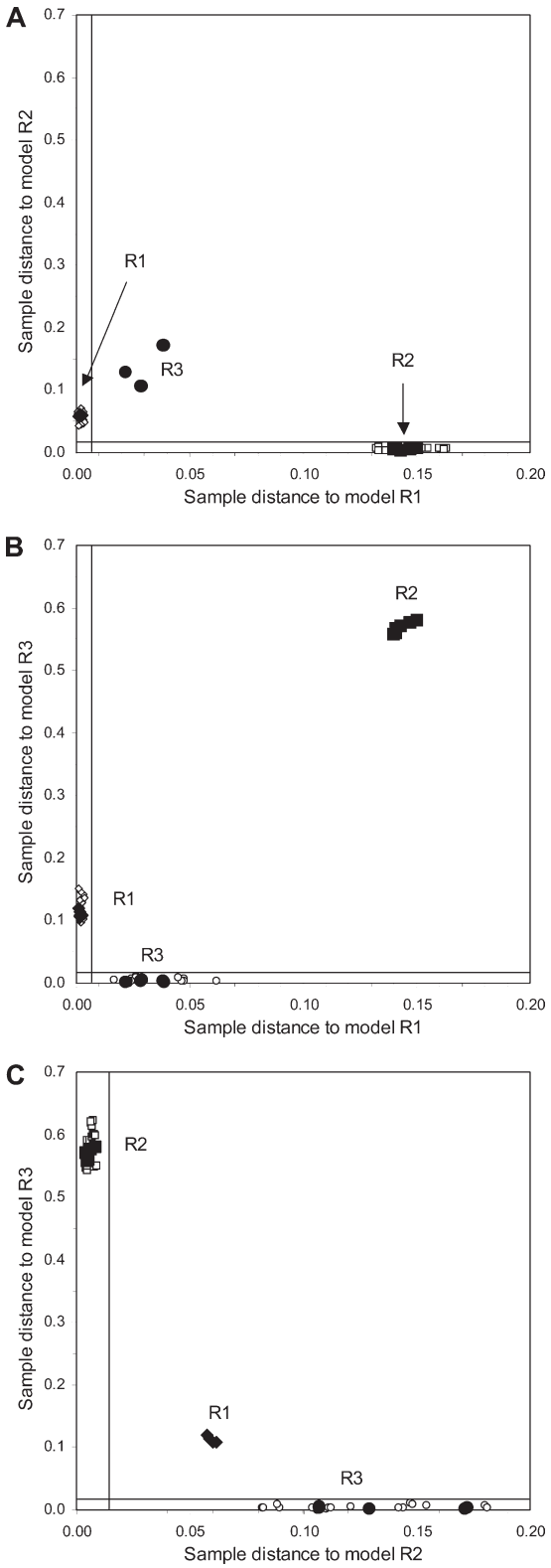

Figure 6. A–C: Cooman's plots of the SIMCA model (2 PCs) for the three resins R1, R2, and R3 based on all NIR spectra in the wavenumber range from 10,000–4160 cm^{-1}. The filled symbols represent the samples used for classification (TS2) on a significance level of 5%. The horizontal and vertical lines in the graphs represent the confidence limits.

between them (R1 + R2 and R3), possibly due to the fact that only one polycondensation step was performed for R3, are visible [Figure 5(C)].

Classification Using Soft Independent Modeling of Class Analogy (SIMCA) and Model Validation

A separate full cross-validated model was created for each resin requiring 2 PCs for each resin to satisfactorily describe each data set. Models for R1, R2, and R3 explain 99.8%, 99.5%, and 99.8% of the data, respectively. The significance level was set to 5%. The Cooman's plots used for SIMCA validation are shown for all class models, as well as the classification of the test set samples (TS2) of each resin formulation (Figure 6). Spectra of the test set samples (TS2) from each resin formulation fall into the membership limits, confirming a correct classification. The distances from SIMCA class R1 to class R2 is 586 and from R1 to class R3 is 398. The big values for these distances are partly due to the baseline differences between the resins. The large distances confirm the applicability of the NIR spectroscopic pattern to unequivocally distinguish different resin formulations.

PLS-R Models for MIR and NIR Spectra

The data set was divided into 28 cross validation (CV) and 6 test set (TS1) samples. Additionally 8 samples were used as a second test set (TS2). The MIR-based PLS-R models were calculated using the offset-corrected spectra (cp. experimental details, data processing). The model statistics are summed up in Table III. The NIR-based PLS-R models were calculated using the 1st derivative + vector normalization preprocessed spectra. The wavenumber range was restricted to two ranges from 7502 to 5446 and 4902 to 4158 cm^{-1}. This was done on one hand to avoid the noisy higher wavenumber range and on the other hand to exclude the range of the water band at which the energy of the transmitted infrared radiation was almost zero, especially for the resin R2. The model statistics are summed up in Table III.

To prove the robustness of the MIR-based PLS-R model, the number of samples left out during cross validation was increased to 25 (of 34) resulting in the following statistics: R^2 = 96%, RMSECV = 0.03 and 3 PLS factors. For the NIR-based PLS-R models the number of samples left out during cross validation was increased up to 25 (of 34) resulting in the following statistics: R^2 = 98%, RMSECV = 0.02 and 2 PLS factors.

Taking into account that the usual molar ratio of this type of resins, when industrially produced, is close to 1.1, a narrower *F/U* ratio range was investigated, namely 1.00–1.20. The results (Table III) demonstrate that the models are of similar quality, although only 21 samples were available for this *F/U* range and the number of PLS factors was halved.

From an analytical point of view (in accordance with AACC Method 39-00[47]), the RPD should be in the following range: ≥2.5 screening in breeding programs; ≥5 acceptable for quality control; ≥8 good for process control, development, and applied research.[47] It has to be kept in mind that the RPD is only correct and comparable when data are normally distributed.

The high RPDs (Table III) obtained for the MIR and NIR models allow drawing the conclusion that the models are applicable for at-line as well as on-line (in-line) process control.

Table III. PLS-R Model Statistics for MIR and NIR

Range of *F/U* ratio	0.9–1.49	
CV (28)[a]/TS1 (6)	MIR	NIR
No. of PLS factors	6	4
R^2 (%) CV	99.9	99.8
RMSECV	0.005	0.007
RPD	30	21
Bias	−0.00016	0.0004
R^2 (%) TS1	99.98	99.9
RMSEP (TS1)	0.003	0.007
RPD (TS1)	73	29
Bias	0.0008	0.002
CVall (34)[a]/TS2 (8)	MIR	NIR
No. of PLS factors	6	4
R^2 (%) CVall	99.9	99.8
RMSECV	0.005	0.007
RPD	34	25
Bias	−0.0001	0.0001
R^2 (%) TS2	99.9	99.8
RMSEP (TS2)	0.003	0.004
RPD (TS2)	34	25
Bias	0.00004	−0.0003
Range of F/U ratio	1.00–1.20	
CV (21)[a]	MIR	NIR
No. of PLS factors	3	2
R^2 (%) CV	99.3	99.5
RMSECV	0.005	0.005
RPD	12	13
Bias	0.0001	0.000008

MIR, spectra offset-corrected (cp. experimental details, data processing), wavenumber range 1780–880 cm^{-1}; NIR: 1st derivative + vector normalization, 2 ranges 7502–5446 cm^{-1} + 4902–4158 cm^{-1}.
[a]Number of samples in brackets.

ATR-MIR (ATR-FTIR) could mainly be used at-line to check the process intermediates and end product or off-line for quality control of outgoing and incoming products in the laboratory. Additionally ATR-MIR can be used for developing processes using MIR fiber optic ATR probes in a laboratory scale reactor[48] were the problems mentioned in the introduction (limited length of the optical fibers, material of the ATR crystal, and especially the fouling of the ATR crystal) can be handled. When ATR-MIR is used at- or off-line the number of samples required to calibrate the instrument can be as low as 20 (15 for calibration and 5 for validation of the method) depending on the variability of the samples and the required precision. Additionally the problem of varying temperatures that appear in the process during resin production is not an issue at- or off-line.

The obtained NIR models with high RPDs and low errors are promising that NIR could by applicable for in-line process control in the context of process analytical technology (PAT). However, the complexity of a real industrial process and

environment has to be taken into account and as the spectra have been collected off-line the model cannot be used for evaluation of the process directly in a reactor, because e.g., spectra from intermediates that are produced during the process and the different temperatures appearing during the resin production have not been taken into account. Especially the latter one is known to influence the NIR spectra[49–52] not only in the range of the combination water band at about 5180 cm^{-1} and in the range of the first overtone of the O-H stretching vibration including the hydrogen bonds (7200–6400 cm^{-1}). The influence of the temperature on the NIR spectra would increase the number of spectra required for calibration. However, although it has been shown that temperature-induced spectral variations can be corrected,[53] this influence could be eliminated by using a small temperature-controlled by-pass with a transmission probe instead of immersing the fiber probe directly into the reactor.

CONCLUSIONS

Applying PCA to the spectra (MIR and NIR) allowed to separate the samples according to the molar ratio and to distinguish between two groups of resins. Soft independent modeling of class analogy (SIMCA) allowed classification of new resin samples with model distances between the classes up to 586.

On the basis of the knowledge acquired during this study, one can suggest that only a few samples (15–20) are necessary to calibrate ATR-FTIR. This means that a method for the determination of the *F/U* molar ratio can be obtained fast and with low costs. PLS-R models based on either MIR or NIR spectra lead to high R^2, low RMSECV and low RMSEP, and high RPDs. The double validation of the results by including a further independent sample set revealed that the process is highly reproducible and that developed models are stable.

Both ATR-FTIR and FT-NIR spectroscopic techniques fulfill the need for classification as well as prediction of samples covering (a) a wide range of *F/U* molar ratios, (b) a narrower range of *F/U* molar ratios, and (c) different resin formulations. The results from this work also suggest that PLS-R models may be used to control the molar ratio of the resin product as part of the process analytical technology (PAT) of the process control on-line (in-line) (FT-NIR) immersing the transmission probe directly in the reactor or at-line (ATR-FTIR) during the resin preparation in industrial processes. Moreover, especially ATR-FTIR could also be a suitable tool for quality control of the incoming resin.

ACKNOWLEDGMENTS

The authors thank Dias de Sousa (Dias de Sousa, Alcochete, Portugal) for supplying the FT-NIR process-spectrometer Matrix-F (Bruker) and Dr. Letícia Andrade for helping in the acquisition of the NIR spectra.

REFERENCES

1. Frihart, C. In Handbook of Wood Chemistry and Wood Composites; Rowell, R., Ed.; CRC Press: Florida, **2005.**
2. Kumlin, K.; Simonson, R. *Angew Makromol. Chem.* **1978,** *68*, 175.
3. Kumlin, K.; Simonson, R. *Angew Makromol. Chem.* **1978,** *72*, 67.
4. Kumlin, K.; Simonson, R. *Angew Makromol. Chem.* **1980,** *86*, 143.
5. Kumlin, K.; Simonson, R. *Angew Makromol. Chem.* **1981,** *93*, 27.
6. Christjanson, P.; Pehk, T.; Siimer, K. *Proc Estonian Acad. Sci. Chem.* **2006,** *55*, 212.
7. Socrates, G. Infrared and Raman Characteristic Group Frequencies. Tables and Charts; Wiley: Chichester, **2001.**
8. Williams, P.; Norris, K. Near-Infrared technology in the agricultural and food industries; American Association of Cereal Chemists: St. Paul, **2004.**
9. Shenk, J. S.; Workman, J. J.; Westerhaus, M. O. In Handbook of Near-Infrared Analysis; Burns, D. A.; Ciurczak, E. W., Eds.; Marcel Dekker: New York, **2001.**
10. Tsuchikawa, S. *Appl. Spectrosc. Rev.* **2007,** *42*, 43.
11. Tsuchikawa, S.; Schwanninger, M. *Appl. Spectrosc. Rev.* **2011,** DOI:10.1080/05704928.2011.621079.
12. Workman, J. J. *Appl. Spectrosc. Rev.* **1999,** *34*, 1.
13. Gierlinger, N.; Jacques, D.; Schwanninger, M.; Wimmer, R.; Hinterstoisser, B.; Pâques, L. E. *Can. J. For Res.* **2003,** *33*, 1727.
14. Gierlinger, N.; Schwanninger, M.; Hinterstoisser, B.; Wimmer, R. *J. Near Infrared Spectrosc.* **2002,** *10*, 203.
15. Fackler, K.; Schwanninger, M.; Gradinger, C.; Hinterstoisser, B.; Messner, K. *FEMS Microbiol. Lett.* **2007,** *271*, 162.
16. Fackler, K.; Schwanninger, M.; Gradinger, C.; Srebotnik, E.; Hinterstoisser, B.; Messner, K. *Holzforschung* **2007,** *61*, 680.
17. Schimleck, L. R.; Evans, R.; Matheson, A. C. *J. Wood Sci.* **2002,** *48*, 132.
18. Schimleck, L. R.; Tyson, J. A.; Jones, P. D.; Peter, G. F.; Daniels, R. F. A. C. III. *J. Near Infrared Spectrosc.* **2007,** *15*, 261.
19. Smidt, E.; Meissl, K.; Schwanninger, M.; Lechner, P. *Waste Manage* **2008,** *28*, 1699.
20. Schwanninger, M.; Hinterstoisser, B.; Gradinger, C.; Messner, K.; Fackler, K. *J. Near Infrared Spectrosc.* **2004,** *12*, 397.
21. Meissl, K.; Smidt, E.; Schwanninger, M. *Talanta* **2007,** *72*, 791.
22. Meissl, K.; Smidt, E.; Schwanninger, M.; Tintner, J. *Appl Spectrosc* **2008,** *62*, 873.
23. Wise, J. K.; Smith, C. D. *Anal. Chem.* **1967,** *39*, 1702.
24. Zorba, T.; Papadopoulou, E.; Hatjiissaak, A.; Paraskevopoulos, K. M.; Chrissafis, K. *J. Therm. Anal. Calorim.* **2008,** *92*, 29.
25. Myers, G. E. *J. Appl. Polym. Sci.* **1981,** *26*, 747.
26. Kandelbauer, A.; Despres, A.; Pizzi, A.; Taudes, I. *J. Appl. Polym. Sci.* **2007,** *106*, 2192.
27. Li, A. P.; Kan, C. Y.; Du, Y.; Liu, D. S. *Acta Phys-Chim Sin* **2006,** *22*, 873.
28. Park, B. D.; Kim, Y. S.; Singh, A. P.; Lim, K. P. *J. Appl. Polym. Sci.* **2003,** *88*, 2677.
29. Chow, S. *Holzforschung* **1977,** *31*, 200.

30. Chow, S.; Steiner, P. R. *Holzforschung* **1978,** *32*, 120.
31. Cosco, S.; Ambrogi, V.; Musto, P.; Carfagna, C. *J. Appl. Polym. Sci.* **2007,** *105*, 1400.
32. Poljansek, I.; Sebenik, U.; Krajnc, M. *J. Appl. Polym. Sci.* **2006,** *99*, 2016.
33. Kemppi, A. *Pap Puu-Pap Tim* **1997,** *79*, 496.
34. Raval, D. K.; Narola, B. N.; Patel, A. J. *Iran Polym. J.* **2005,** *14*, 775.
35. Dessipri, E.; Minopoulou, E.; Chryssikos, G. D.; Gionis, V.; Paipetis, A.; Panayiotou, C. *Eur. Polym. J.* **2003,** *39*, 1533.
36. Minopoulou, E.; Dessipri, E.; Chryssikos, G. D.; Gionis, V.; Paipetis, A.; Panayiotou, C. *Int. J. Adhes. Adhes.* **2003,** *23*, 473.
37. Blanco, M.; Villaescusa, V. *Talanta* **2007,** *71*, 1333.
38. Dessipri, E., Chryssikos, G., Gionis, V., Paipetis, A., Kalousis, G., inventor; Use of NIR (Near-Infrared spectroscopy) in composite panel production WO/2002/051898, **2002** 04.07.2002.
39. Savitzky, A.; Golay, M. J. E. *Anal. Chem.* **1964,** *36*, 1627.
40. Esbensen, K. H. Multivariate Data Analysis—In practice. An Introduction to Multivariate Data Analysis and Experimental Design; CAMO Process AS: Oslo, **2002.**
41. Schwanninger, M.; Rodrigues, J. C.; Gierlinger, N.; Hinterstoisser, B. *J. Near Infrared. Spectrosc.* **2011,** *19*, 331.
42. Schwanninger, M.; Rodrigues, J. C.; Gierlinger, N.; Hinterstoisser, B. *J. Near Infrared Spectrosc.* **2011,** *19*, 319.
43. Jada, S. S. *J. Appl. Polym. Sci.* **1988,** *35*, 1573.
44. Mauer, L. J.; Chernyshova, A. A.; Hiatt, A.; Deering, A.; Davis, R. *J. Agric. Food Chem.* **2009,** *57*, 3974.
45. Holopainen, H.; Alvila, L.; Pakkanen, T. T.; Rainio, J. *J. Appl. Polym. Sci.* **2003,** *89*, 3582.
46. Workman, J.; Weyer, L. Practical Guide to Interpretive Near-Infrared Spectroscopy; CRC Press: New York, **2007.**
47. AACC. American Association of Cereal Chemists (AACC): **1999,** p 15.
48. Poljansek, I.; Krajnc, M. *Acta Chim. Slov* **2005,** *52*, 238.
49. Czarnik-Matusewicz, B.; Pilorz, S. *Vib Spectrosc.* **2006,** *40*, 235.
50. Czarnik-Matusewicz, B.; Pilorz, S.; Hawranek, J. P. *Anal. Chim. Acta.* **2005,** *544*, 15.
51. Maeda, H.; Ozaki, Y.; Tanaka, M.; Hayashi, N.; Kojima, T. *J. Near Infrared Spectrosc.* **1995,** *3*, 191.
52. Segtnan, V. H.; Sasic, S.; Isaksson, T.; Ozaki, Y. *Anal. Chem.* **2001,** *73*, 3153.
53. Wülfert, F.; Kok, W. T.; de Noord, O. E.; Smilde, A. K. *Anal. Chem.* **2000,** *72*, 1639.